The flavoprotein FOXRED2 reductively activates nitro-chloromethylbenzindolines and other hypoxia-targeting prodrugs

Francis W. Hunter[a], Jagdish K. Jaiswal[a], Daniel G. Hurley[b,c 1], H. D. Sarath Liyanage[a], Sarah P. McManaway[a], Yongchuan Gu[a], Susan Richter[a 2], Jingli Wang[a], Moana Tercel[a,c], Cristin G. Print[b,c], William R. Wilson[a,c], Frederik B. Pruijn[a,c]

Authors' Affiliations: [a]Auckland Cancer Society Research Centre, Faculty of Medical and Health Sciences, and [b]Department of Molecular Medicine and Pathology and Bioinformatics Institute, and [c]Maurice Wilkins Centre for Molecular Biodiscovery, University of Auckland, Private Bag 92019, Auckland 1142, New Zealand.

F W Hunter: f.hunter@auckland.ac.nz, J K Jaiswal: j.jaiswal@auckland.ac.nz, D G Hurley: daniel.hurley@unimelb.edu.au, H D S Liyanage: sarath.liyanage@auckland.ac.nz, S P McManaway: s.mcmanaway@auckland.ac.nz, Y Gu: y.gu@auckland.ac.nz, S Richter: susan.richter2@uniklinikum-dresden.de, J Wang: jingli.wang@auckland.ac.nz, M Tercel: m.tercel@auckland.ac.nz, C G Print: c.print@auckland.ac.nz, W R Wilson: wr.wilson@auckland.ac.nz, F B Pruijn: f.pruijn@auckland.ac.nz

Corresponding author: Frederik B Pruijn, f.pruijn@auckland.ac.nz, Auckland Cancer Society Research Centre, University of Auckland, Private Bag 92019, Auckland 1142, New Zealand. Phone: +64-9-923 6939. Fax: +64-9-3737 502. E-mail: f.pruijn@auckland.ac.nz.

[1] Current address: Systems Biology Laboratory, Melbourne School of Engineering, and NICTA Victoria Research Laboratory, the University of Melbourne.

[2] Current address: Institute for Clinical Chemistry and Laboratory Medicine, University Hospital Carl Gustav Carus Dresden, Dresden University of Technology.

ABSTRACT

The nitro-chloromethylbenzindoline prodrug SN29428 has been rationally designed to target tumour hypoxia. SN29428 is metabolised to a DNA minor groove alkylator via oxygen-sensitive reductive activation initiated by unknown one-electron reductases. The present study sought to identify reductases capable of activating SN29428 in tumours. Expression of candidate reductases in cell lines was modulated using forced expression and, for P450 (cytochrome) oxidoreductase (POR), by zinc finger nuclease-mediated gene knockout. Affymetrix microarray mRNA expression of flavoreductases was correlated with SN29428 activation in a panel of 23 cancer cell lines. Reductive activation and cytotoxicity of prodrugs were measured using mass spectrometry and antiproliferative assays, respectively. SN29428 activation under hypoxia was strongly attenuated by the *pan*-flavoprotein inhibitor diphenyliodonium, but less so by knockout of *POR* suggesting other flavoreductases contribute. Forced expression of 5-methyltetrahydrofolate-homocysteine methyltransferase reductase (*MTRR*), as well as *POR*, increased activation of SN29428 in hypoxic HCT 116 cells. SN29428 activation strongly correlated with expression of *POR* and also FAD-dependent oxidoreductase domain containing 2 (*FOXRED2*), in cancer cell lines. This association persisted after removing the effect of POR enzyme activity using first-order partial correlation. Forced expression of *FOXRED2* increased SN29428 activation and cytotoxicity in hypoxic HEK293 cells and also increased activation of hypoxia-targeted prodrugs PR-104A, tirapazamine and SN30000, and increased cytotoxicity of the clinical-stage prodrug TH-302. Thus this study has identified three flavoreductases capable of enzymatically activating SN29428, one of which (FOXRED2) has not previously been implicated in xenobiotic metabolism. These results will inform future development of biomarkers predictive of SN29428 sensitivity.

Keywords: FOXRED2, nitroCBI, TH-302, PR-104, hypoxia-targeting prodrug, tirapazamine

1. Introduction

Hypoxia is a prevalent feature of solid malignancies that arises as a result of structural and functional irregularities in tumour microvasculature. It is a uniquely attractive target for cancer therapy due to its severity in tumours and its functional contributions to disease progression and resistance to several modes of therapy [1-3]. Such considerations have led to the rational development of hypoxia-activated prodrugs (HAPs) that are designed to exploit tumour hypoxia. These prodrugs are metabolised to cytotoxic species – principally DNA-damaging agents – via enzyme-catalysed reductive reactions that are suppressed by molecular oxygen. Examples of HAPs that are currently in clinical or advanced preclinical development include nitro aromatic compounds TH-302 [4] and PR-104 [5], and the aromatic *N*-oxide SN30000 [6] which is an improved analogue of the well-studied HAP tirapazamine (TPZ) [7].

We have reported on the development of nitro-chloromethylbenzindolines [8, 9], a novel chemical class of HAP derived from the bacterial cyclopropylindoline antibiotics, which monoalkylate *N3* of adenine in a sequence-selective manner in the DNA minor groove. These natural products and their derivatives have been explored as potential anticancer agents; however, myelotoxicity of the four analogues (adozelesin, bizelesin, carzelesin and KW-2189) that were evaluated in clinical trials precluded dosing at levels consistent with antitumour activity in xenograft models [10]. Cyclopropylindolines nonetheless possess a number of desirable pharmacological properties including extremely high cytotoxic potency [11, 12]. To seek additional tumour selectivity, we developed synthetic analogues of cyclopropylindolines in which the phenol group of the alkylating moiety is replaced by an amino group (amino-chloromethylbenzindolines; aminoCBIs) [13-15]. These derivatives retain the key features of the earlier phenolic compounds [15, 16] but also allow for the cognate nitro compound (nitro-chloromethylbenzindoline; nitroCBI) to function as a HAP by

virtue of an initial oxygen-sensitive one-electron reduction step that ultimately generates the cytotoxic aminoCBI. The strongly electron-withdrawing nitro group in nitroCBIs prevents DNA alkylation, attenuating cytotoxicity, and nitroCBIs are therefore relatively non-toxic compounds. An early experimental nitroCBI was up to 300-fold more potent under hypoxia than normoxia, >500-fold less toxic to mice than the corresponding aminoCBI and selectively killed hypoxic cells in RIF-1 xenografts at its maximum tolerated dose (MTD) [9]. A more recent lead in the nitroCBI series, SN29428 (see Fig. 1 for structure), was 10- to 250-fold more toxic to human tumour cell lines under hypoxia than normoxia [8]. The corresponding phosphate pre-prodrug showed systemic release of SN29428 and caused selective killing of radiation-resistant hypoxic cells in SiHa and HCT 116 xenografts with tumour growth delay at non-toxic doses, whereas the cognate aminoCBI was inactive [8]. NitroCBI therefore represent a promising new class of HAP that is currently in preclinical development.

HAPs exploit a complex biological target, with utility dependent on multiple requirements being met simultaneously including the presence of hypoxia, intrinsic sensitivity to the active metabolite and expression of reductases that are capable of activating the prodrug in hypoxic cells. Initially, HAPs are reduced to a prodrug radical intermediate by one-electron reductases. In the presence of oxygen this radical is rapidly re-oxidised to regenerate the parent prodrug, thereby suppressing subsequent formation of the cytotoxic metabolite. Conversely, rearrangement of the initial prodrug radical intermediate or its further reduction in poorly-oxygenated cells results in selective formation of cytotoxic metabolites in hypoxic tumour regions. Identifying reductases capable of catalysing the initial one-electron reduction is therefore a critical objective toward developing predictive biomarkers for defining patient groups who are likely to respond to HAP therapy. Although the identity of reductases capable of activating nitroCBIs have not been investigated in detail, other HAPs including PR-104A [17, 18], TPZ and SN30000 [19] appear to be metabolised primarily by flavoreductases,

which catalyse two-electron transfer between NAD(P)H donors to FAD and FMN cofactors that then mediate one-electron transfer to substrates. Small molecule HAPs with one-electron reduction potentials comparable to those of flavin nucleotides can function as exogenous electron acceptors and intercept single electrons from the reduced cofactors [20]. Known HAP-activating flavoreductases include P450 (cytochrome) oxidoreductase (POR), NADPH-dependent diflavin oxidoreductase 1 (NDOR1), inducible nitric-oxide synthase (NOS2A), 5-methyltetrahydrofolate-homocysteine methyltransferase reductase (MTRR) and cytochrome b5 reductase 3 [17, 18, 21, 22]. In addition, some HAPs are substrates for specific two-electron reductases, which typically mediate oxygen-insensitive bioreductive activation. For instance, apaziquone (EO9) is activated by NADH:quinone oxidoreductase-1 (NQO1, DT-diaphorase) [23] and PR-104A is a substrate for aldo-keto reductase family 1 member C3 (AKR1C3) [24]. Although this two-electron activation compromises hypoxic selectivity, it can also potentially be exploited in tumours with high expression of these reductases.

With the exception of AKR1C3, identification of HAP reductases has largely relied on studies with purified enzymes or evaluation of individual candidates in panels of stably transfected cell lines. Such studies have identified reductases capable of enzymatic HAP activation, but are low-throughput approaches that do not directly interrogate the activity of candidates at endogenous levels of expression. We present here the first comprehensive investigation of nitroCBI-activating reductases in hypoxic human cancer cells using an alternative, rational bioinformatic approach. The correlation of the abundance of oxidoreductase RNA transcripts with metabolic activation of SN29428 in 23 human cancer cell lines under hypoxia suggested FAD-dependent oxidoreductase domain containing 2 (FOXRED2; also known as endoplasmic reticulum flavoprotein associated with degradation or ERFAD [25]) as a candidate HAP reductase. This prediction was tested using forced expression of FOXRED2 in HEK293 cells, which confirmed the ability of FOXRED2 to activate SN29428 and other

HAPs under hypoxia. Conventional screening in a panel of stably transfected HCT 116 cell lines also identified POR and MTRR to be capable of activating SN29428. These results will inform subsequent development of biomarkers for predicting activity of nitroCBI reductases in clinical settings.

2. MATERIALS AND METHODS

2.1. Compounds

SN29428 [8], TH-302 [26], SN30000 [6], TPZ [27] and PR-104A [26] were synthesised at the Auckland Cancer Society Research Centre as reported. Drugs were stored as stock solutions in DMSO (SN29428, TH-302, PR-104A), or saline (TPZ, SN30000) at −80 °C. Synthesis of tetra-deuterated SN29428 and SN29932 (aminoCBI) [28], tetra-deuterated PR-104A and its reduced metabolites PR-104H and PR-104M [29], and octa-deuterated SN30000, TPZ and their respective 1-oxide and nor-oxide metabolites has been reported [30]. Diphenyliodonium (DPI) and DMSO were purchased from Sigma-Aldrich, St Louis, MO.

2.2. Cell lines

HCT 116 cell lines with stable expression of POR, MTRR, CYB5R3, NOS2A, FDXR, NQO1, AKR1C1, AKR1C2, AKR1C3 and XDH have been reported [17]. HEK293 cells stably expressing full-length FOXRED2 protein containing C-terminal hexa-His and FLAG tags (3B2B cells, designated herein HEK293-FOXRED2) [25], and the isogenic HEK293-Host line, were obtained from the University of Copenhagen. The establishment and characterisation of SiHa lines with genetic knockout of *POR* are detailed elsewhere [21]; the SiHa-POR$^{-/-}$ clone used here is named S2ko1 in the latter study. A summary of the wild type tumour lines used in this study and their origins is provided in Table 1. Cells were cultured as previously described [17, 18, 25] for <6 months cumulative passage from frozen stocks that were authenticated by short tandem repeat DNA profiling in our laboratory by Dr E Leung using a Genescan kit (SiHa, H460, HCT116), or at CellBank Australia (H1299, HEPG2, HT29) or by the supplier (ATCC or ECACC, see Table 1) except for A549, FaDu, HEK293,

MDA-MB-231, PC3 and Skov3 which were not authenticated. All lines were confirmed to be *Mycoplasma*-free by PCR-ELISA (Roche Diagnostics).

2.3. Liquid chromatography-mass spectrometry assays of HAP metabolism

Drug exposures for assaying *in vitro* metabolism of SN29428 were performed in 96-well plates as previously [28], except that in the case of the panel of 23 wild type tumour lines and the library of oxidoreductase-expressing HCT 116 cells (Tables 1 and 2, respectively) cultures were scaled up to 400 μL in 24-well format. Briefly, cells were seeded in plates under aerobic or hypoxic (H_2/Pd-scrubbed anaerobic chamber, Coy Laboratory Products; <10 ppm O_2 gas phase using plasticware and medium pre-equilibrated for 3 d) conditions and allowed to settle for 2 h before exposing to SN29428 for 4 h. For DPI treatment, cells were exposed to 100 μM DPI 1 h prior to and during SN29428 treatment. After drug exposure, plates were immediately placed on ice and the whole culture was deproteinised with four volumes of ice-cold acetonitrile (Merck, Billerica MA) containing tetra-deuterated SN29428 and SN29932 (aminoCBI) as internal standards. Samples were stored at −80 °C until analysis by single-quadrupole LC-MS (SiHa, SiHa-POR$^{-/-}$, HEK293-FOXRED2 and HEK293-Host) or triple-quadrupole LC-MS/MS (23-cell line panel and HCT 116 library).

For LC-MS, samples were analysed for SN29428 and its reduced aminoCBI metabolite using an Agilent series 1100 liquid chromatography instrument coupled with an Agilent 6150 single-quadrupole mass spectrometer (Agilent Technologies, Santa Clara, CA). Acetonitrile extracts were centrifuged (12 000 *g* at room temperature for 5 min) and the supernatant was reduced to 50 μL using a vacuum evaporator, then reconstituted with 100 μL 1:2 acetonitrile-aqueous ammonium formate buffer (0.45 M, pH 4.5). These samples were centrifuged again prior to injecting 100 μL into the instrument from an autosampler. Chromatographic separation was achieved using an Alltima C8 column (2.1 × 150 mm, 5 μm) with a 45 mM

aqueous ammonium formate (Sigma-Aldrich) buffer (pH 4.5) /80% acetonitrile gradient (Table 3) with a flow rate of 0.3 mL.min^{-1} and a run time of 16 min. Ionisation was achieved using electrospray ionisation in positive mode with a fragmentation voltage of 75 V. Selected ion monitoring was performed at m/z values of 620 ([D_4]SN29428 internal standard), 616 (SN29428), 590 ([D_4]SN29932 internal standard) and 586 (SN29932).

For LC-MS/MS, samples were analysed using an Agilent 6410 Triple Quadrupole LC-MS/MS system (Agilent Technologies). Acetonitrile extracts were centrifuged (12 000 *g* at room temperature for 5 min) and 100 µL samples of supernatant were evaporated to dryness then reconstituted in 0.01% formic acid (Sigma-Aldrich). Samples of 25 µL were injected into the instrument from an autosampler. Chromatographic separation was achieved using a Zorbax column (SB-C18, 2.1 × 30 mm, 3.5 µm) at 30 °C and a 0.01% aqueous formic acid/CH_3CN gradient (Table 4) with a flow rate of 0.5 mL.min^{-1} and run time of 7 min. Ionisation was achieved using multimode ionisation with a gas temperature of 350 °C, vaporiser 200 °C and gas flow rate 6 L.min^{-1}, nebuliser pressure 40 psi and capillary voltage 3.5 kV. For both bioanalytical methods, calibration curves were generated by spiking tetra-deuterated internal standards of SN29428 and aminoCBI into samples of medium from control wells (cells without drug) for final concentrations of 0.001 – 2.5 µM. Standards were extracted in acetonitrile and reconstituted in formic acid in the same manner as experimental samples.

In vitro metabolism of SN30000, TPZ and PR-104A was assayed using validated LC-MS/MS methods as described earlier [29-31].

2.4. Gene expression arrays and data analysis

Microarray data (Affymetrix HG-U133 Plus 2.0 arrays) for global gene expression in a panel of 23 log-phase human cancer cell lines (Table 1), which were obtained previously in this laboratory [24], were retrieved from the Array Express repository (Expt ID:E-TABM-767). The Affymetrix .CEL files were pre-processed and normalised using the 'affy' package [32] in the statistical programming language R (http://cran.r-project.org/). Quality control using the 'AffyQCReport' function showed that the data were of good quality with no obvious outlying chips. The data were normalised using the RMA method [33] and exported and saved to tab-delimited text format for further analysis. Pearson correlations and partial Pearson correlations between transcript abundance data and phenotypic measures – principally one-electron metabolism of prodrugs, which we defined as the difference between metabolism under hypoxic conditions and aerobic conditions – were computed using the 'cor' and 'pcor' functions, respectively, in the 'ggm' package [34]. Missing data were handled by using case-wise deletion. Partial Pearson correlations were conditioned on POR activity in S9 fractions of cell lysates, measured as cyanide-resistant NADPH-dependent cytochrome c reductase activity, which we have reported elsewhere for this cell line panel [19, 35]. Empirical *P*-values for the correlations and partial correlations were estimated by permuting (randomly rearranging) the data 100 times for each distribution and calculating the same correlations on the permuted data. Correlation values in the 95^{th} or 99^{th} percentiles based on the permuted data were inferred *P*-values of $P < 0.05$ or $P < 0.01$, respectively, for the experimental data.

2.5. Cytotoxicity assays

Sensitivity of cell lines to prodrugs was evaluated by assaying antiproliferative potency. Cells were seeded in 96-well plates at a density of 3000 cells/0.1 mL and exposed to compounds at varying concentrations for 4 h under aerobic or hypoxic (<10 ppm O_2, as above) conditions.

Medium composition for drug incubation was αMEM containing 10% foetal calf serum, 200 μM 2'-deoxycytidine (Sigma-Aldrich) and 17 mM D-glucose (Gibco, Life Technologies). Drug exposure was terminated by washing, after which cells were cultured for 4 days in air/CO_2 before staining with sulphorhodamine B (Sigma-Aldrich). IC_{50} values were calculated by interpolation, using 4-parameter logistic regression, as the drug concentration reducing staining to 50% of untreated controls on the same plate.

2.6. Western immunoblotting

For FOXRED2 immunoblotting, cell lysates were harvested in radioimmunoprecipitation assay buffer and protein concentration was measured by bicinchoninic acid assay. Twenty five micrograms of protein was resolved on 4-12% gradient SDS-PAGE gels (Invitrogen), transferred to PVDF membrane, blocked, and probed with anti-FOXRED2 (rabbit polyclonal HPA031611, Sigma-Aldrich, 1:2000 dilution) or anti-actin (mouse monoclonal MAB1501R, Chemicon, 1:5000 dilution) primary antibodies overnight at 4 ºC. After incubation with secondary antibody (sc-2055, Santa Cruz Biotechnology, Dallas, TX), membranes were imaged using ECL chemiluminescence detection (Thermo Scientific). POR immunoblotting was performed as before [26].

2.7. Statistics

Statistical tests, with the exception of high-throughput computations relating to gene expression data which were performed in R as described above, were undertaken using SigmaPlot 11.2 (Systat Software, Inc.). * denotes $P < 0.05$, ** denotes $P < 0.01$, *** denotes $P < 0.001$.

3. Results

3.1. SN29428 is metabolised by flavoreductases in hypoxic cells

Bioreductive prodrugs of chemical classes unrelated to the nitroCBIs, including the dinitrobenzamide mustard PR-104A and the benzotriazine di-*N*-oxide SN30000, are activated in hypoxic cells primarily via single-electron reduction by NAD(P)H-dependent flavoreductases with low substrate specificity as xenobiotic metabolising enzymes [17-19]. To evaluate whether nitroCBIs are also activated by flavoreductases, we compared reductive metabolism of SN29428 to the cognate aminoCBI in hypoxic SiHa cervical carcinoma cells in the presence or absence of the irreversible *pan*-flavoenzyme inhibitor DPI [36, 37]. DPI treatment inhibited 86 ± 0.1% (mean ± SEM) of total aminoCBI production at the concentration tested (Fig. 2A), which suggested that flavoreductases are indeed the predominant class of activating enzymes in this cell line.

To identify specific enzymes that are capable of reducing nitroCBIs, we measured hypoxic and aerobic metabolism of SN29428 in a previously-reported panel of 10 stably-transfected HCT 116 pools that express flavoreductases and members of aldo-keto reductase family 1C (Fig. 2B and Table 2). This candidate-based screen identified that forced expression of the diflavin reductases POR and MTRR increased activation of SN29428 under hypoxic conditions by 3.5- and 2.5-fold above wild type HCT 116 cells, respectively. Notably, SN29428 was not a substrate for NOS2A, which reduces both PR-104A [17] and SN30000 [19] under hypoxic conditions. Importantly, aerobic metabolism was not significantly increased in cell lines overexpressing the known aerobic (i.e. two-electron) nitroreductases NQO1 and AKR1C3 (Welch's *t*-test; $P > 0.05$).

These data suggested that expression of POR may play a role in nitroCBI activation in hypoxic tumour cells. To quantitate the contribution of endogenous POR to total SN29428 activation, we compared bioreductive metabolism in wild type SiHa cells to an isogenic clone in which *POR* was deleted using zinc finger nuclease technology [21] (Fig. 2C). Genetic knockout of *POR* significantly reduced DPI-sensitive metabolism in cells exposed to 10 μM SN29428 under hypoxic conditions (Fig. 2D). This phenotype was confirmed in an independent experiment (Fig. 2E); however, both experiments showed residual DPI-sensitive SN29428 metabolism in the *POR* knockout line. Interestingly, deletion of *POR* did not reduce bioreductive metabolism when cells were exposed 0.1 or 1 μM SN29428 (Fig. 2E). Taken together, these results demonstrate a role for POR in metabolic activation of SN29428 in SiHa cells but also establish that it is not the sole flavoreductase that activates SN29428 in this cell line.

3.2. Metabolism of SN29428 correlates with POR and with FOXRED2 expression in tumour cell lines

To characterise nitroCBI activation in a wider sample of human tumour cell lines, we measured metabolism of SN29428 under hypoxic and aerobic conditions in a panel of 23 genetically diverse human cell lines representing multiple tumour types (Fig. 3A). Activation of SN29428 was suppressed by oxygen 5- to 80-fold in these cell lines, with 17-fold variation in total aminoCBI production under hypoxia across the panel. There was a positive association between formation of aminoCBI under hypoxic conditions and enzymatic activity of POR measured as NADPH-dependent, cyanide-resistant reduction of cytochrome c (Pearson correlation r = 0.632, $P = 0.002$; Fig. 3B).

To identify additional reductases that may contribute to metabolism of nitroCBI prodrugs under hypoxic conditions, we compared the metabolism data with Affymetrix microarray

mRNA expression profiles in the same cell lines. We computed Pearson correlations between normalised abundance of 54 675 probe sets representing 19 701 unique RNAs and: (i) SN29428 metabolism under hypoxia or (ii) hypoxic metabolism of SN29428 net of aerobic metabolism (i.e. oxygen-inhibitable one-electron metabolism). To specifically identify flavoreductases, we filtered the list of correlations to retain all descendants of the gene ontology nodes 'FAD or $FADH_2$ binding' (GO:0050660) or 'flavin mononucleotide binding' (GO:0010181), which yielded a list of 181 probe sets corresponding to 79 unique genes. The resulting list was ranked by descending value of correlation coefficient and the top 20 correlating probes are given in Table 5. This algorithm revealed the top-ranking candidate to be *FOXRED2* (*ERFAD*), which encodes for an ER-luminal flavoprotein that contains consensus motifs for binding the redox cofactors NADPH and FAD [25] but has not previously been described to possess xenobiotic metabolising activity or to be a DPI-sensitive flavoenzyme. All three probe sets specific for *FOXRED2* mRNA that are represented on the Affymetrix HG-U133 Plus 2.0 chips were significantly correlated with one-electron metabolism of SN29428 (Fig. 4A-C). Of these *FOXRED2* correlations, two coefficients were beyond the empirical threshold for $P < 0.01$ ($r = 0.528$) as estimated by permutation analysis (random rearrangement of the data to estimate correlations produced by chance alone as described in 'Materials and Methods').

To directly evaluate which of these correlating flavoproteins are most likely to contribute to variability in oxygen-sensitive SN29428 metabolism that is not explained by POR activity, we explicitly removed the effect of POR by computing first-order partial Pearson correlations conditioned on enzymatic activity of POR in S9 fractions of cell lysates. A number of flavoproteins that were strongly correlated with SN29428 metabolism prior to conditioning, including the single probe set for *POR* itself, lost this association after conditioning on POR activity (Fig. 4D-E). Conversely, all three probe sets specific for *FOXRED2* RNA remained

strongly correlated with SN29428 activation after the effect of POR was removed, and *FOXRED2* again yielded the single highest correlating probe set of all RNAs encoding flavoproteins (Table 6). In order to assess the association between SN29428 metabolism and abundance of flavoprotein RNAs using a method that equally weights any monotonic relationship, we repeated these computations using Spearman rank correlation in place of the Pearson method. In agreement with the Pearson correlations, this analysis identified probe sets specific for *FOXRED2* RNA to be the most strongly correlated of all flavoprotein RNAs with SN29428 metabolism both before and after conditioning on POR activity (data not shown). These results identified FOXRED2 as a priority candidate nitroCBI reductase for experimental validation.

3.3. FOXRED2 increases SN29428 metabolism and cytotoxicity in hypoxic cells

To test the hypothesis that FOXRED2 is a *bona fide* nitroCBI reductase, we obtained a HEK293 cell line that had been stably transfected to express full-length FOXRED2 with C-terminal hexa-His and FLAG tags (HEK293-FOXRED2; Fig. 5A). Expression of FOXRED2 increased metabolic activation of SN29428 by 2.3-fold compared to the isogenic HEK293-Host line under hypoxic conditions, but did not affect SN29428 activation in aerobic cells (Fig. 5B). Notably, this increase in hypoxic metabolism was abrogated by treating with DPI, which confirmed that the mechanism of nitroCBI activation is true flavin-dependent enzymatic reduction. This elevated SN29428 activation was associated with a concomitant 3.5-fold increase in antiproliferative potency under hypoxia (Fig. 5C) but no change in potency under aerobic conditions (Fig. 5D). These gain-of-function results clearly demonstrate that FOXRED2 is a nitroCBI reductase capable of increasing oxygen-sensitive metabolism and inhibition of cell growth.

3.4. FOXRED2 activates the bioreductive prodrugs SN30000, TPZ and PR-104A and increases cytotoxicity of TH-302

HAP-activating flavoreductases identified to date appear to be broadly capable of metabolising agents belonging to several distinct chemical classes [17, 19, 26, 35]. To investigate whether FOXRED2 shares this low substrate specificity as a one-electron xenobiotic reductase, we compared activation and/or antiproliferative potency of clinical- or near-clinical stage HAPs SN30000, TPZ, PR-104A and TH-302 in HEK293-FOXRED2 and HEK293-Host cells. Expression of FOXRED2 increased metabolism of the two closely-related benzotriazine *N*-oxide HAPs SN30000 and TPZ across a range of prodrug concentrations under hypoxic conditions (Fig. 6A-B), with no change in metabolism under aerobic conditions (data not shown). Interestingly, this increase in SN30000 activation did not concomitantly elevate antiproliferative potency (Fig. 6C-D). Expression of FOXRED2 similarly increased oxygen-sensitive activation of the dinitrobenzamide mustard PR-104A by 1.7-fold (Fig. 6E). This was associated with an oxygen-sensitive 2.0-fold increase in antiproliferative potency of this agent (Fig. 6F). We next examined the effects of FOXRED2 expression on the antiproliferative potency of the most clinically-advanced HAP – the 2-nitroimidazole mustard TH-302. Expression of FOXRED2 increased cell sensitivity to TH-302 by 3.8-fold under aerobic conditions and 2.3-fold under hypoxic conditions (Fig. 6F), respectively. Collectively these data suggest that FOXRED2 is a *bona fide* HAP reductase that may contribute to the activation of clinically important HAPs in hypoxic tumour cells.

4. Discussion

We demonstrate here that metabolic activation of nitroCBIs, a promising new class of HAPs currently in lead optimisation stage, is dependent on enzymatic activity of flavoreductases. Forced expression of candidates in HCT 116 cells identified two enzymes competent for nitroCBI activation – the diflavin reductases POR and MTRR – that have also been implicated in the metabolism of other HAPs [17, 19]. The central discovery of this study, that FOXRED2 is also a HAP flavoreductase, arose from an extension of the gene expression profiling strategy that had been used to identify AKR1C3 as an aerobic PR-104A two-electron reductase [24]. The present approach is novel in the sense that it sought to identify oxygen-sensitive one-electron reductases, which is a significantly more challenging undertaking given the apparent contribution of multiple reductases to hypoxic activation of HAPs.

The observation that SN29428 is activated primarily by DPI-sensitive flavoproteins in hypoxic SiHa cells is consistent with analogous observations for HAPs of different chemical classes [4, 17, 19]. Indeed POR and MTRR have both been reported to be capable of reductively activating PR-104A [17, 18], TPZ and the 2-nitroimidazole hypoxia probe EF5 [19], and forced expression of POR has also recently been shown to sensitise HCT 116 and SiHa cells to SN29428 in independent studies from our group [21]. This suggests that the cohort of enzymes responsible for metabolism of nitroCBI prodrugs overlap those for the dinitrobenzamide mustards, *N*-oxides and 2-nitroimidazoles, although there appear to be some distinct differences. For example, in the present study, SN29428 is not a substrate for NOS2A although the same NOS2A-overexpressing HCT 116 line demonstrates increased activation of PR-104A [17], SN30000 and EF5 [19] and the 6-nitroquinolone FSL-61 [35]. In further support of a considerable overlap in reductase profile for HAP activation under hypoxia, we

found that FOXRED2 is also capable of oxygen-sensitive activation of SN30000, TPZ, PR-104A and increases cytotoxicity of TH-302 under both hypoxic and aerobic conditions. The latter observation agrees with our earlier finding and by others that forced expression of POR potentiates aerobic as well as hypoxic cytotoxicity of TH-302 [4, 26]. The apparent homology in reductive activation across chemical classes implies that [^{18}F]-fluorinated derivatives of bioreductive 2-nitroimidazole probes, such as EF5, fluoromisonidazole, HX4 and FAZA could serve as PET biomarkers of both tumour hypoxia and HAP reductase activity in clinical settings [30], although it will be important to evaluate critically whether this match is sufficient to make these probes generically useful as predictive biomarkers for HAP one-electron reductases.

The residual DPI-sensitive SN29428 activation we observed in SiHa-POR$^{-/-}$ cells confirmed that additional flavoreductases contribute to HAP activation in this cell line, and is consistent with the lack of resistance of *POR* knockout HCT 116 and SiHa clones to SN29428 under anoxia we reported recently [21]. The lack of effect on cytotoxicity in the latter study is consistent with the lack of effect on SN29428 metabolism at low SN29428 concentrations (0.1 and 1 μM; Fig. 2E) given that its hypoxic IC_{50} is in the range 0.07 – 0.18 μM in the parental and POR knockout cell lines [21]. The identification of FOXRED2 as a novel nitroCBI-activating flavoprotein demonstrates the potential of the bioinformatic approach despite the significant functional redundancy in enzymatic reduction of HAPs. FOXRED2, also known as ERFAD, is an ER-luminal flavoprotein that has been ascribed a role in elimination of misfolded proteins by interacting with components of the ER-associated degradation (ERAD) pathway [25, 38]. FOXRED2 has also been implicated in amyloid β-mediated neuronal cell death through inhibition of the 26S proteasome and enhanced ER stress [39]. Increased expression of ERAD pathway elements, which are mediated by activation of the unfolded protein response, is a key feature of tumour cell adaptation to

hypoxia [40]. It will be interesting to determine whether FOXRED2 expression is modified in hypoxic tumour regions. FOXRED2 associates with FAD and also contains a consensus sequence for NADPH binding [25], although no enzymatic activity has been reported. This study therefore constitutes the first demonstration that FOXRED2 is a DPI-sensitive flavoenzyme capable of reducing exogenous substrates.

While we have shown that FOXRED2 is capable of activating HAPs of multiple chemical classes, HAP activation inside the ER lumen, where FOXRED2 is localised, appears to constitute a cytotoxic event only in the case of prodrugs that generate stable, lipophilic metabolites capable of diffusing across lipid membranes. FOXRED2 may therefore be a valid target for HAPs that exert bystander cell killing (i.e. killing of neighbouring metabolically incompetent cells), which potentially include nitroCBIs [9], dinitrobenzamide mustards such as PR-104A [41] and 2-nitroimidazole mustards such as TH-302 [4]. This implies that FOXRED2 would not augment the therapeutic activity of the benzotriazine *N*-oxides SN30000 and TPZ, the cytotoxic metabolites of which are considered to be short-lived oxidising radicals [42] that are likely to be membrane impermeable. This interpretation is consistent with the unchanged hypoxic cytotoxicity of SN30000 in the HEK293 cell line that stably expressed high levels of FOXRED2 compared to wild type.

FOXRED2 mRNA appears to be widely and highly expressed in human tumours. A survey of Gene Expression Omnibus (GEO; www.ncbi.nlm.nih.gov/geo) identified the same 231846_at probe set used in the present study to indicate transcript abundance greater than the median on Affymetrix microarrays for 58/58 surgical non-small cell lung cancer specimens (range 53rd-90th percentile; median 71st percentile; Experiment ID 62816801), 37/62 colorectal cancers (60%; range 34th-78th percentile; median 52nd percentile; Experiment ID 84995901), and in 47/47 basal-like breast cancers (range 53rd-90th percentile; median 71st percentile; Experiment

ID 28993201). Hypoxia has recently been implicated in the pathogenicity of basal-like and triple-negative breast cancer [43-47] and it has been suggested that HAPs may be an promising therapeutic strategy for these tumours [48]. Notably, *FOXRED2* transcripts were also above the median abundance in 39/39 pancreatic ductal adenocarcinomas (range 51st-69th percentile; median 60th percentile; Experiment ID 78922701), which is an indication for which TH-302 is currently undergoing Phase 3 evaluation. We also note that median-normalised *FOXRED2* transcript abundance in our 23-cell line panel was in a similar range (range 58th-90th percentile; median 74th percentile; 231846_at probe set) to that in the above patient tumour samples. Given that FOXRED2 is enzymatically capable of reductively activating HAPs, this suggests that FOXRED2 is likely to contribute to prodrug activation in some human tumours.

Tumour hypoxia is among the best validated therapeutic targets yet to be directly exploited by an approved clinical agent, with the possible exception of the DNA crosslinking agent mitomycin c, which is mildly selective for hypoxic cells [49]. The long-standing goal of drugging hypoxia has arguably been confounded by failure to align the pharmacology and clinical development strategy of experimental HAPs with the requirements of this complex target, for which biomarker-driven drug development faces hurdles similar to those for polytargeted anticancer compounds [50]. Identifying HAP reductases such as FOXRED2 is an important component of developing integrated clinical biomarker sets predictive of HAP sensitivity of individual tumours. However, although FOXRED2 is widely expressed in human tumours, whether it is a significant determinant of HAP sensitivity *in vivo* is yet to be assessed. RNAi-mediated knockdown of *FOXRED2* in SiHa cells gave equivocal effects on SN29428 activation (data not shown). This highlights the challenge of establishing culpability of individual oxidoreductases using loss-of-function techniques in a functionally redundant system, and is consistent with earlier reports that antagonism of POR by RNAi or genetic

knockout in many cases does not significantly suppress HAP activation [18, 21]. Thus measuring expression of single reductases is unlikely to be sufficient for predicting HAP activation in tumours; rather, multiplexed interrogation of panels of enzymes will be required. We recently reported development of a proteotypic peptide mass spectrometry method for measuring concentrations of specific tryptic peptides (initially POR) in tumour lysates [21], which is potentially amenable to quantifying reductase sets in tumour biopsies [51]. Identifying the HAP-activating reductases that will feature on these panels is a key first step toward development of such predictive tools for supporting translation of HAPs in the clinic.

Acknowledgements

This research was supported by grants from the Cancer Society, Auckland; the Foundation for Research, Science and Technology (UOAX0703); the Health Research Council of New Zealand (grants 11/1103 and 12/529) and by scholarships from the Genesis Oncology Trust and the University of Auckland (awarded to F W Hunter). We thank Dr Michael Hay for synthesis of SN30000, TPZ and TH-302, Huai-Ling Hsu for assistance with mass spectrometry and Drs Lars Ellgaard, Adam Patterson, Chris Guise and Jiechuang Su for provision of cell lines.

Conflict of interest

W R Wilson and F B Pruijn are named as inventors on patents relating to SN30000. W R Wilson is named as an inventor on patents relating to PR-104. All other authors have no conflict of interest.

References

[1] Wilson WR, Hay MP. Targeting hypoxia in cancer therapy. Nat Rev Cancer. 2011;11:393-410.

[2] Shannon AM, Bouchier-Hayes DJ, Condron CM, Toomey D. Tumour hypoxia, chemotherapeutic resistance and hypoxia-related therapies. Cancer Treat Rev. 2003;29:297-307.

[3] Vaupel P, Mayer A. Hypoxia in cancer: Significance and impact on clinical outcome. Cancer Metastasis Rev. 2007;26:225-39.

[4] Meng F, Evans JW, Bhupathi D, Banica M, Lan L, Lorente G, et al. Molecular and cellular pharmacology of the hypoxia-activated prodrug TH-302. Mol Cancer Ther. 2012;11:740-51.

[5] Patterson AV, Ferry DM, Edmunds SJ, Gu Y, Singleton RS, Patel K, et al. Mechanism of action and preclinical antitumor activity of the novel hypoxia-activated DNA cross-linking agent PR-104. Clin Cancer Res. 2007;13:3922-32.

[6] Hicks KO, Siim BG, Jaiswal JK, Pruijn FB, Fraser AM, Patel R, et al. Pharmacokinetic/pharmacodynamic modeling identifies SN30000 and SN29751 as tirapazamine analogues with improved tissue penetration and hypoxic cell killing in tumors. Clin Cancer Res. 2010;16:4946-57.

[7] Zeman EM, Brown JM, Lemmon MJ, Hirst VK, Lee WW. SR-4233: A new bioreductive agent with high selective toxicity for hypoxic mammalian cells. Int J Radiat Oncol Biol Phys. 1986;12:1239-42.

[8] Tercel M, Atwell GJ, Yang S, Ashoorzadeh A, Stevenson RJ, Botting KJ, et al. Selective treatment of hypoxic tumor cells in vivo: Phosphate pre-prodrugs of nitro analogues of the duocarmycins. Ang Chem Int Ed. 2011;50:2606-9.

[9] Wilson WR, Stribbling SM, Pruijn FB, Syddall SP, Patterson AV, Liyanage HDS, et al. Nitro-chloromethylbenzindolines: Hypoxia-activated prodrugs of potent adenine N3 DNA minor groove alkylators. Mol Cancer Ther. 2009;8:2903-13.

[10] Pavlidis N, Aamdal S, Awada A, Calvert H, Fumoleau P, Sorio R, et al. Carzelesin phase II study in advanced breast, ovarian, colorectal, gastric, head and neck cancer, non-Hodgkin's lymphoma and

malignant melanoma: A study of the EORTC early clinical studies group (ECSG). Cancer Chemother and Pharmacol. 2000;46:167-71.

[11] Boger DL, Johnson DS. CC-1065 and the duocarmycins: Understanding their biological function through mechanistic studies. Angew Chem Int Ed. 1996;35:1439-74.

[12] Tichenor MS, Boger DL. Yatakemycin: Total synthesis, DNA alkylation, and biological properties. Nat Prod Rep. 2008;25:220-6.

[13] Tercel M, Denny WA, Wilson WR. Nitrogen and sulfur analogues of the seco-CI alkylating agent: Synthesis and cytotoxicity. Bioorg Med Chem Lett. 1996;6:2735-40.

[14] Atwell GJ, Tercel M, Boyd M, Wilson WR, Denny WA. Synthesis and cytotoxicity of 5-amino-1-(chloromethyl)-3-[(5,6,7- trimethoxyindol-2-yl)carbonyl], 1,2 dihydro-3H-benz[e]indole (Amino-seco- CBI-TMI) and related 5-alkylamino analogues: New DNA minor groove alkylating agents. J Org Chem. 1998;63:9414-20.

[15] Tercel M, Gieseg MA, Denny WA, Wilson WR. Synthesis and cytotoxicity of amino-seco-DSA: An amino analogue of the DNA alkylating agent duocarmycin SA. J Org Chem. 1999;64:5946-53.

[16] Gieseg MA, Matejovic J, Denny WA. Comparison of the patterns of DNA alkylation by phenol and amino seco-CBI-TMI compounds: Use of a PCR method for the facile preparation of single end-labelled double-stranded DNA. Anticancer Drug Des. 1999;14:77-84.

[17] Guise CP, Abbattista MR, Tipparaju SR, Lambie NK, Su J, Li D, et al. Diflavin oxidoreductases activate the bioreductive prodrug PR-104A under hypoxia. Mol Pharmacol. 2012;81:31-40.

[18] Guise CP, Wang AT, Theil A, Bridewell DJ, Wilson WR, Patterson AV. Identification of human reductases that activate the dinitrobenzamide mustard prodrug PR-104A: A role for NADPH:cytochrome P450 oxidoreductase under hypoxia. Biochem Pharmacol. 2007;74:810-20.

[19] Wang J, Guise CP, Hsu H-L, Hurley D, Wilson WR, Patterson AV. Abstract 2111: Identification of reductases capable of metabolic activation of hypoxia targeting prodrug SN30000 and hypoxia marker EF5. AACR 104th Annual Meeting 2013. 2013.

[20] Wardman P. Electron transfer and oxidative stress as key factors in the design of drugs selectively active in hypoxia. Curr Med Chem. 2001;8:739-61.

[21] Su J, Gu Y, Pruijn FB, Smaill JB, Patterson AV, Guise CP, et al. Zinc finger nuclease knockout of NADPH:cytochrome P450 oxidoreductase (POR) in human tumour cell lines demonstrates that hypoxia-activated prodrugs differ in POR dependence. J Biol Chem. 2013;288:37138-53.

[22] Seow HA, Penketh PG, Shyam K, Rockwell S, Sartorelli AC. 1,2-Bis(methylsulfonyl)-1-(2-chloroethyl)-2-[[1-(4-nitrophenyl)ethoxy] carbonyl]hydrazine: An anticancer agent targeting hypoxic cells. Proc Natl Acad Sci USA. 2005;102:9282-7.

[23] Gustafson DL, Beall HD, Bolton EM, Ross D, Waldren CA. Expression of human NAD(P)H:quinone oxidoreductase (DT-diaphorase) in Chinese hamster ovary cells: Effect on the toxicity of antitumor quinones. Mol Pharmacol. 1996;50:728-35.

[24] Guise CP, Abbattista MR, Singleton RS, Holford SD, Connolly J, Dachs GU, et al. The bioreductive prodrug PR-104A is activated under aerobic conditions by human aldo-keto reductase 1C3. Cancer Res. 2010;70:1573-84.

[25] Riemer J, Appenzeller-Herzog C, Johansson L, Bodenmiller B, Hartmann-Petersen R, Ellgaard L. A luminal flavoprotein in endoplasmic reticulum-associated degradation. Proc Natl Acad Sci. 2009;106:14831-6.

[26] Hunter FW, Wang J, Patel R, Hsu HL, Hickey AJR, Hay MP, et al. Homologous recombination repair-dependent cytotoxicity of the benzotriazine di-N-oxide CEN-209: Comparison with other hypoxia-activated prodrugs. Biochem Pharmacol. 2012;83:574-85.

[27] Boyd M, Hay MP, Boyd PDW. Complete 1H, 13C and 15N NMR assignment of tirapazamine and related 1,2,4-benzotriazine N-oxides. Magn Reson Chem. 2006;44:948-54.

[28] Tercel M, Lee HH, Yang S, Liyanage HDS, Mehta SY, Boyd PDW, et al. Preparation and antitumour properties of the enantiomers of a hypoxia-selective nitro analogue of the duocarmycins. ChemMedChem. 2011;6:1860-71.

[29] Gu Y, Patterson AV, Atwell GJ, Chernikova SB, Brown JM, Thompson LH, et al. Roles of DNA repair and reductase activity in the cytotoxicity of the hypoxia-activated dinitrobenzamide mustard PR-104A. Mol Cancer Ther. 2009;8:1714-23.

[30] Wang J, Foehrenbacher A, Su J, Patel R, Hay MP, Hicks KO, et al. The 2-nitroimidazole EF5 is a biomarker for oxidoreductases that activate the bioreductive prodrug CEN-209 under hypoxia. Clin Cancer Res. 2012;18:1684-95.

[31] Gu Y, Wilson WR. Rapid and sensitive ultra-high-pressure liquid chromatography-tandem mass spectrometry analysis of the novel anticancer agent PR-104 and its major metabolites in human plasma: Application to a pharmacokinetic study. J Chromat B, Analyt Technol Biomed Life Sci. 2009;877:3181-6.

[32] Gentleman RC, Carey VJ, Bates DM, Bolstad B, Dettling M, Dudoit S, et al. Bioconductor: open software development for computational biology and bioinformatics. Genome Biol. 2004;5.

[33] Irizarry RA, Bolstad BM, Collin F, Cope LM, Hobbs B, Speed TP. Summaries of Affymetrix GeneChip probe level data. Nucleic Acids Res. 2003;31.

[34] Marchetti GM. Independencies induced from a graphical Markov model after marginalization and conditioning: the R package ggm. J Stat Softw. 2006;15:1-15.

[35] Su J, Guise CP, Wilson WR. FSL-61 is a 6-nitroquinolone fluorogenic probe for one-electron reductases in hypoxic cells. Biochem J. 2013;452:79-86.

[36] Tew DG. Inhibition of cytochrome P450 reductase by the diphenyliodonium cation. Kinetic analysis and covalent modifications. Biochemistry. 1993;32:10209-15.

[37] O'Donnell VB, Smith GCM, Jones OTG. Involvement of phenyl radicals in iodonium compound inhibition of flavoenzymes. Mol Pharmacol. 1994;46:778-85.

[38] Riemer J, Hansen HG, Appenzeller-Herzog C, Johansson L, Ellgaard L. Identification of the PDI-family member ERp90 as an interaction partner of ERFAD. PLoS ONE. 2011;6.

[39] Shim S, Lee W, Chung H, Jung YK. Amyloid β-induced FOXRED2 mediates neuronal cell death via inhibition of proteasome activity. Cell Mol Life Sci. 2011;68:2115-27.

[40] Wouters BG, Koritzinsky M. Hypoxia signalling through mTOR and the unfolded protein response in cancer. Nat Rev Cancer. 2008;8:851-64.

[41] Wilson WR, Hicks KO, Pullen SM, Ferry DM, Helsby NA, Patterson AV. Bystander effects of bioreductive drugs: Potential for exploiting pathological tumor hypoxia with dinitrobenzamide mustards. Rad Res. 2007;167:625-36.

[42] Anderson RF, Shinde SS, Hay MP, Gamage SA, Denny WA. Activation of 3-amino-1,2,4-benzotriazine 1,4-dioxide antitumor agents to oxidizing species following their one-electron reduction. J Am Chem Soc. 2003;125:748-56.

[43] Tan EY, Yan M, Campo L, Han C, Takano E, Turley H, et al. The key hypoxia regulated gene CAIX is upregulated in basal-like breast tumours and is associated with resistance to chemotherapy. Br J Cancer. 2009;100:405-11.

[44] Voss MJ, Möller MF, Powe DG, Niggemann B, Zänker KS, Entschladen F. Luminal and basal-like breast cancer cells show increased migration induced by hypoxia, mediated by an autocrine mechanism. BMC Cancer. 2011;11.

[45] Neumeister VM, Sullivan CA, Lindner R, Lezon-Geyda K, Li J, Zavada J, et al. Hypoxia-induced protein CAIX is associated with somatic loss of BRCA1 protein and pathway activity in triple negative breast cancer. Breast Cancer Res Treat. 2012;136:67-75.

[46] Dong C, Yuan T, Wu Y, Wang Y, Fan TM, Miriyala S, et al. Loss of FBP1 by Snail-mediated repression provides metabolic advantages in basal-like breast cancer. Cancer Cell. 2013.

[47] Network TCGA. Comprehensive molecular portraits of human breast tumours. Nature. 2012;490:61-70.

[48] Zardavas D, Baselga J, Piccart M. Emerging targeted agents in metastatic breast cancer. Nat Rev Clin Oncol. 2013;10:191-210.

[49] Teicher BA, Lazo JS, Sartorelli AC. Classification of antineoplastic agents by their selective toxicities toward oxygenated and hypoxic tumor cells. Cancer Res. 1981;41:73-81.

[50] Jonsson B, Bergh J. Hurdles in anticancer drug development from a regulatory perspective. Nat Rev Clin Oncol. 2012;9:236-43.

[51] Takadate T, Onogawa T, Fukuda T, Motoi F, Suzuki T, Fujii K, et al. Novel prognostic protein markers of resectable pancreatic cancer identified by coupled shotgun and targeted proteomics using formalin-fixed paraffin-embedded tissues. Int J Cancer. 2013;132:1368-82.

Figure Legends

Fig. 1. (A) Chemical structure of the nitroCBI prodrug SN29428 and its cognate aminoCBI metabolite SN29932. (B) Mechanism of activation of nitroCBIs via one-electron reduction to a free radical intermediate that is reoxidised to the initial prodrug in the presence of oxygen or further reduced to the amine in its absence. The amine spontaneously cyclises to a cyclopropyl intermediate that alkylates the *N*3 position of adenine leading to cytotoxicity.

Fig. 2. SN29428 is activated by flavoreductases under hypoxic conditions. (A) Small molecule flavoprotein inhibitor DPI (100 μM; added 1 h prior to SN29428) abrogates SN29428 metabolism in hypoxic SiHa cells. Cells were exposed to 1 μM SN29428 for 4 h and metabolism is shown as the amount of SN29932 per cell detected in growth medium at cessation of exposure, expressed as % of SiHa cells not treated with DPI. Values are mean + standard error of 3 independent cultures. (B) Metabolism of SN29428 in HCT 116 cell lines with stable forced expression of oxidoreductases under hypoxic and aerobic conditions. Cells were exposed for 4 h to 10 μM SN29428. One-electron metabolism was defined as metabolism under hypoxic conditions net of metabolism under aerobic conditions. Metabolism is expressed as the amount of aminoCBI metabolite per cell detected in growth medium at the cessation of SN29428 exposure. Values are mean + standard error of ≥ 3 experiments. Statistical comparisons are for one-electron metabolism compared to HCT 116 wild type (hatched bar). (C) Confirmation of POR protein depletion in SiHa-POR$^{-/-}$ cells by Western immunoblotting. The blot shown is representative of multiple independent experiments performed while characterising SiHa-POR$^{-/-}$ in our laboratory [21]. (D) SN29428 metabolism in SiHa wild type and SiHa-POR$^{-/-}$ cells with or without DPI treatment. Cells were exposed to 10 μM SN29428 for 4 h in the presence or absence of 100 μM DPI (added 1 h prior to SN29428). Metabolism is expressed as the concentration of aminoCBI in the

extracellular medium at the cessation of drug exposure, and is the mean + standard error of three independent cultures. (E) Metabolism of SN29428 under hypoxic conditions in SiHa wild type and SiHa-POR$^{-/-}$ cells with or without DPI treatment. Cells were exposed to nominal SN29428 concentrations of 0.1, 1 and 10 μM in the presence or absence of 100 μM DPI. Bioreductive metabolism was measured as in (D). For all figures, significance was evaluated using Student's *t*-test.

Fig. 3. Reductive metabolism of SN29428 in a panel of human tumour cell lines. (A) Metabolism of SN29428 in a panel of wild type tumour cell lines under hypoxic and aerobic conditions, determined as in Figure 2B. One-electron metabolism was defined as metabolism under hypoxic conditions net of metabolism under aerobic conditions. Values are mean + standard error of 3 independent experiments each with triplicate cultures. (B) Pearson correlation of one-electron metabolism of SN29428 and POR enzymatic activity (NADPH-dependent, cyanide-resistant cytochrome c reductase activity in S9 preparations) in the panel of 23 tumour cell lines.

Fig. 4. SN29428 activation correlates with *FOXRED2* expression in tumour cells. (A-C) Pearson correlations between one-electron metabolism of SN29428 and abundance of *FOXRED2* mRNA. The latter was evaluated as median-centred log2 expression detected by *FOXRED2*-specific Affymetrix probe sets 231846_at, (A); 220707_s_at, (B); and 233250_x_at, (C). (D) Comparison of the strength of associations between one-electron metabolism of SN29428 and abundance of probes specific for transcripts of flavoproteins before and after removing the known effect of POR activity. The numerical ranking of individual probe sets amongst all probe sets on the chip, based on descending magnitude of Pearson correlation coefficient, is plotted on the abscissa. The equivalent metric, after conditioning on POR biochemical activity using first-order partial correlation, is shown on the

ordinate. The long dashed-dotted diagonal line gives the function $f(x) = \mathrm{y}$ and deviation from this line reflects changes in association strength after conditioning the correlations on POR activity. The short dashed horizontal and vertical lines indicate the thresholds above which *P*-values are inferred to be less than 0.01. The probe sets specific for *FOXRED2* and *POR* (208928_at) are shown as filled triangles and square, respectively. (E) Re-scaled version of (D) to clearly distinguish the probe sets specific for *FOXRED2* and *POR*.

Fig. 5. FOXRED2 expression increases activation and cytotoxicity of SN29428 under hypoxic conditions. (A) Confirmation of stable forced expression of FOXRED2 in HEK293 cells by Western immunoblotting. The blot shown is representative of 3 independent experiments. (B) Metabolism of SN29428 in HEK293-FOXRED2 and isogenic HEK293-Host cells with or without DPI treatment (added 1 h prior to SN29428) under hypoxic and aerobic conditions. Cells were exposed to 10 μM SN29428 for 4 h and metabolism is expressed as Figure 2D. Values are intra-experiment mean + standard error of 3 replicate wells and are representative of independent experiments performed. (C-D) Antiproliferative potency of SN29428 (4 h exposure followed by wash-out and growing the cells for 4 days in fresh culture medium) against HEK293-FOXRED2 and HEK293-Host cells under hypoxic (C) and aerobic (D) conditions. The half maximal inhibitory concentrations (IC_{50}) plotted are inter-experiment mean + standard error of 3 independent assays. Significance was evaluated using two-way analysis of variance (ANOVA).

Fig. 6. FOXRED2 activates the bioreductive prodrugs SN30000, TPZ and PR-104A and increases cytotoxicity of TH-302. (A) Metabolism of SN30000 in HEK293-Host and HEK293-FOXRED2 cells under hypoxic conditions. Metabolism is expressed as the rate of SN30000 consumption and production over 4 h of its 1-oxide and nor-oxide metabolites as a function of the measured initial SN30000 concentration. Values are mean + standard error of

6 independent cultures pooled from two experiments. Statistical significance was assessed by two-way ANOVA. (B) Metabolism of TPZ in HEK293-Host and HEK293-FOXRED2 cells under hypoxic conditions, as for SN30000 in panel (A). The nor-oxide metabolite was not present above the detection limit of the assay. Antiproliferative potency of SN30000 in HEK293-FOXRED and HEK293-Host cells under aerobic (C) and hypoxic (D) conditions (4 h exposure followed by wash-out and growing the cells for 4 days in fresh culture medium). Half-maximal inhibitory concentrations (IC_{50}) values shown are inter-experiment means + standard error of 3 independent assays. Statistical significance was tested using two-way ANOVA. (E) Metabolism of PR-104A in HEK293-Host cells ('H') and HEK293-FOXRED2 cells ('F') under aerobic and hypoxic conditions. Metabolism was measured as concentration of the reduced hydroxylamine (PR-104H) and amine (PR-104M) metabolites in the combined intracellular/extracellular fraction after exposing to 100 μM PR-104A for 1 h. Values are mean + standard error of 3 independent cultures. Significance was established with Student's *t*-test using the sum of PR-104H and PR-104M concentrations as the test statistic. (D) Antiproliferative potency of PR-104A and TH-302 against HEK293-Host and HEK293-FOXRED2 cells under aerobic and hypoxic conditions. Values are inter-experiment mean + standard error of 4 (PR-104A) or 3 (TH-302) experiments. Significance was assessed using two-way ANOVA.

Table 1: Panel of 23 human tumour cell lines, types of primary tumour from which the lines were derived and the sources from which they were obtained.

Cell line	Tumour type	Source
22Rv1	Prostate	ATCC
A2780	Ovarian	ECACC
A431	Uterine	ATCC
A549	NSCLC	Dr. J. Martin Brown, Stanford University, USA
C-33 A	Cervix	Onyx Pharmaceuticals, CA
DU 145	Prostate	ATCC
FaDu	H&N	Dr. Mark Dewhirst, Duke University, USA
H1299	NSCLC	Onyx Pharmaceuticals, CA, USA
H460	NSCLC	ATCC
H522	NSCLC	ATCC
H69	SCLC	ATCC
H82	SCLC	ATCC
HCT 116	Colon	ATCC
HCT-8Sa	Colon	ATCC
Hep 3b	Liver	ATCC
Hep G2	Liver	ATCC
HT-29	Colon	Dr. David Ross, U. Colorado, USA
MDA-MB-231	Breast	Dr. Adam Patterson, University of Manchester, UK
MIA PaCa-2	Pancreas	ATCC
PANC-1	Pancreas	ECACC
PC-3	Prostate	Dr. Ronnie Cohen, Perth, Australia
SiHa	Cervix	Dr. David Cowan, Ontario Cancer Institute, Canada
SKOV-3	Ovarian	Dr. Martin Ford, Glaxo-Wellcome, UK

Table 2: Oxidoreductases and flavoreductases expressed in the library of HCT 116 cell lines.

Official Gene Symbol	Full gene name	Description
AKR1C1	Aldo-keto reductase family 1, member C1	Oxidoreductase
AKR1C2	Aldo-keto reductase family 1, member C2	Oxidoreductase
AKR1C3	Aldo-keto reductase family 1, member C3	Oxidoreductase
CYB5R3	Cytochrome b5 reductase 3	Flavoreductase
FDXR	Ferredoxin reductase	Flavoreductase
MTRR	5-methyltetrahydrofolate-homocysteine methyltransferase reductase	Flavoreductase
NOS2A	Nitric oxide synthase 2, inducible	Flavoreductase
NQO1	NAD(P)H dehydrogenase, quinone 1	Flavoreductase
POR	P450 (cytochrome) oxidoreductase	Flavoreductase
XDH	Xanthine dehydrogenase	Flavoreductase

Table 3. HPLC solvent gradients for LC-MS analysis of SN29428 and its reduced metabolite SN29932. The mobile phase comprised 45 mM aqueous ammonium formate buffer (pH 4.5; Solvent A) /80% CH_3CN in water (Solvent B) at a flow rate of 0.3 $mL.min^{-1}$.

Time (min)	Solvent A (%)	Solvent B (%)
0	80	20
8	5	95
14	5	95
16	80	20
22	80	20

Table 4. HPLC solvent gradients for LC-MS/MS analysis of SN29428 and its reduced metabolite SN29932. The mobile phase comprised 0.01% formic acid in water (Solvent A) with increasing concentrations of 0.01% formic acid/CH_3CN (Solvent B) at a flow rate of 0.5 $mL.min^{-1}$.

Time (min)	Solvent A (%)	Solvent B (%)
0	80	20
0.5	80	20
3	20	80
6.5	20	80
7	80	20

Table 5: Highest-ranking 20 probe sets specific for transcripts of flavoproteins correlated with one-electron (i.e. oxygen-sensitive) metabolism of SN29428 by Pearson correlation; ranked by descending magnitude of correlation coefficient. Correlation coefficients for 1% and 5% false discovery rates were 0.5277 and 0.3574, respectively.

Official Gene Symbol	Gene name	Probe ID	r
FOXRED2	FAD-dependent oxidoreductase domain containing 2	231846_at	0.68
MAOB	Monoamine oxidase B	204041_at	0.64
STEAP4	STEAP family member 4	220187_at	0.57
CHDH	Choline dehydrogenase	1559591_s_at	0.57
CHDH	Choline dehydrogenase	1559590_at	0.56
CHDH	Choline dehydrogenase	229954_at	0.56
FOXRED2	FAD-dependent oxidoreductase domain containing 2	220707_s_at	0.55
FMO5	Flavin containing monooxygenase 5	240422_at	0.55
ACADSB	Acyl-CoA dehydrogenase, short/branched chain	205355_at	0.51
FMO5	Flavin containing monooxygenase 5	215300_s_at	0.51
FMO5	Flavin containing monooxygenase 5	205776_at	0.51
DUS2L	Dihydrouridine synthase 2-like, SMM1 homolog (S. cerevisiae)	47105_at	0.48
STEAP4	STEAP family member 4	225987_at	0.48
TXNRD3	Thioredoxin reductase 3	221906_at	0.47
CHDH	Choline dehydrogenase	231994_at	0.46
LDHD	Lactate dehydrogenase D	229241_at	0.46
ETFA	Electron-transfer-flavoprotein, alpha polypeptide	201931_at	0.45
ACOX1	Acyl-CoA oxidase 1, palmitoyl	209601_at	0.45
TXNRD3	Thioredoxin reductase 3	59631_at	0.45
ACOX1	Acyl-CoA oxidase 1, palmitoyl	227962_at	0.45

Table 6: Highest-ranking 20 probe sets specific for transcripts of flavoproteins correlated with one-electron (i.e. oxygen-sensitive) metabolism of SN29428 by first-order partial correlation conditioned on POR activity; ranked by descending magnitude of correlation coefficient. Correlation coefficients for 1% and 5% false discovery rates were 0.5919 and 0.3743, respectively.

Official Gene Symbol	Gene name	Probe ID	r
FOXRED2	FAD-dependent oxidoreductase domain containing 2	231846_at	0.76
STEAP4	STEAP family member 4	220187_at	0.75
TXNRD1	Thioredoxin reductase 1	1561080_at	0.63
DUS2L	Dihydrouridine synthase 2-like, SMM1 homolog (S. cerevisiae)	47105_at	0.63
TXNRD3	Thioredoxin reductase 3	221906_at	0.63
STEAP4	STEAP family member 4	225987_at	0.61
TXNRD3	Thioredoxin reductase 3	59631_at	0.56
SDHA	Succinate dehydrogenase complex, subunit A, flavoprotein (Fp)	201093_x_at	0.54
FOXRED2	FAD-dependent oxidoreductase domain containing 2	220707_s_at	0.52
MAOB	Monoamine oxidase B	204041_at	0.47
COQ6	Coenzyme Q6 homolog, monooxygenase (S. cerevisiae)	218760_at	0.46
MTRR	5-methyltetrahydrofolate-homocysteine methyltransferase reductase	203200_s_at	0.42
TXNRD1	Thioredoxin reductase 1	201266_at	0.42
ETFA	Electron-transfer-flavoprotein, alpha polypeptide	201931_at	0.41
FOXRED2	FAD-dependent oxidoreductase domain containing 2	233250_x_at	0.38
DUS2L	Dihydrouridine synthase 2-like, SMM1 homolog (S. cerevisiae)	219486_at	0.35
ETFDH	Electron-transferring-flavoprotein dehydrogenase	33494_at	0.29
ACADVL	Acyl-CoA dehydrogenase, very long chain	200710_at	0.29
ACAD9	Acyl-CoA dehydrogenase family, member 9	224160_s_at	0.29
AGPS	Alkylglycerone phosphate synthase	225114_at	0.28

Figure 1: Chemical structure of the nitroCBI SN29428 and its cognate aminoCBI metabolite and pathway for prodrug activation leading to cytotoxicity

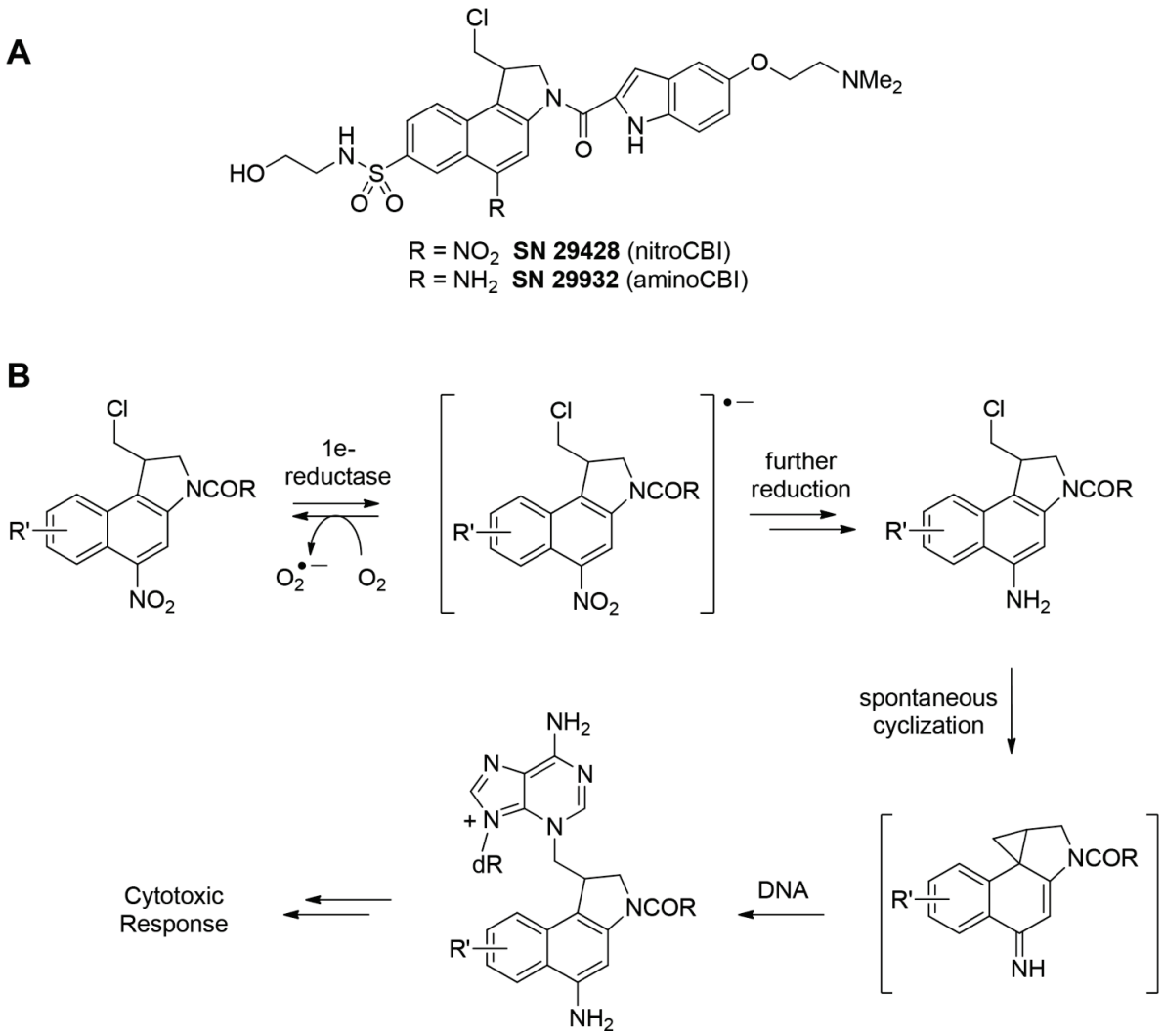

Figure 2: SN29428 is activated by flavoreductases under hypoxic conditions

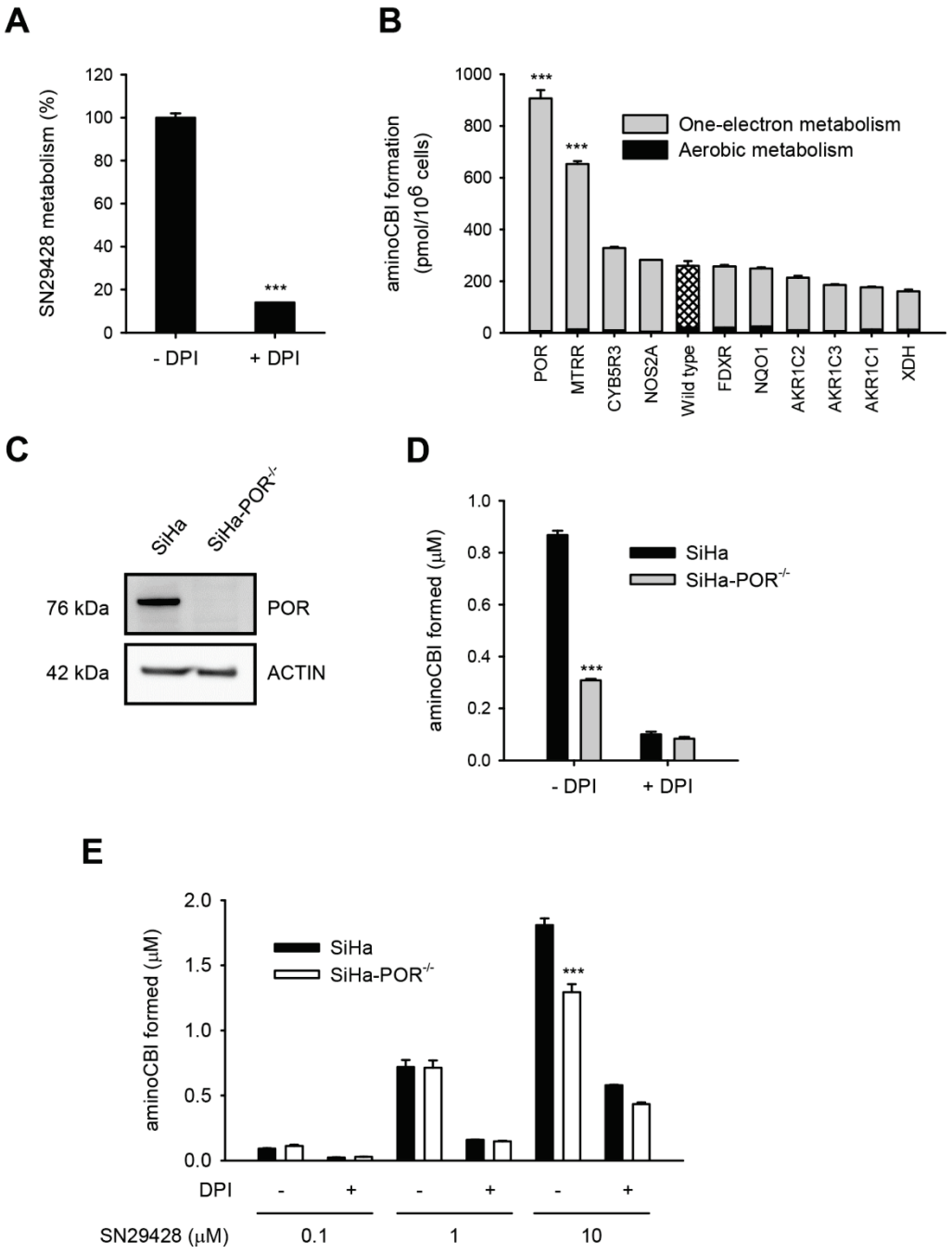

Figure 3: Metabolism of SN29428 in hypoxic tumour cells correlates with POR activity.

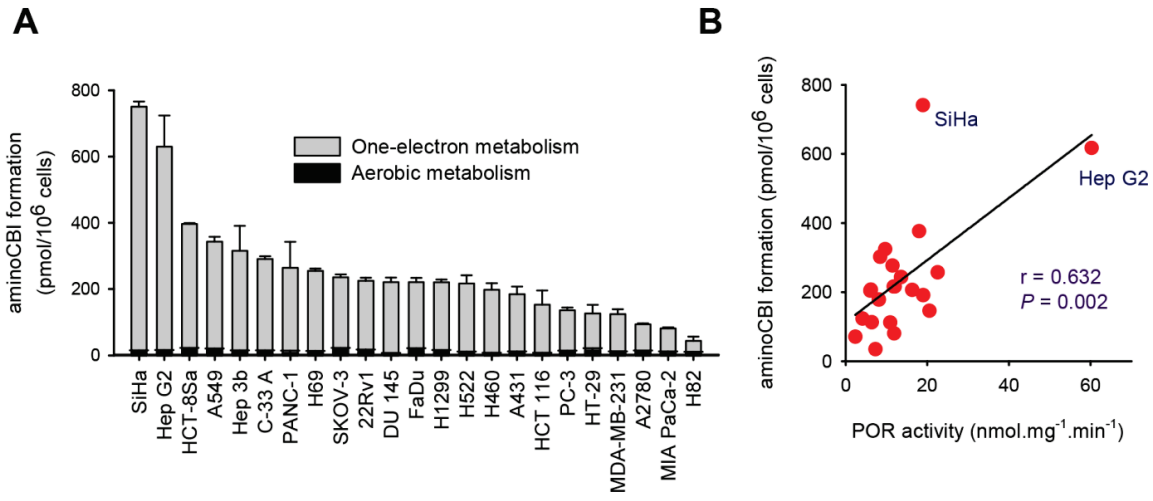

Figure 4: SN29428 activation correlates with *FOXRED2* expression in tumour cells.

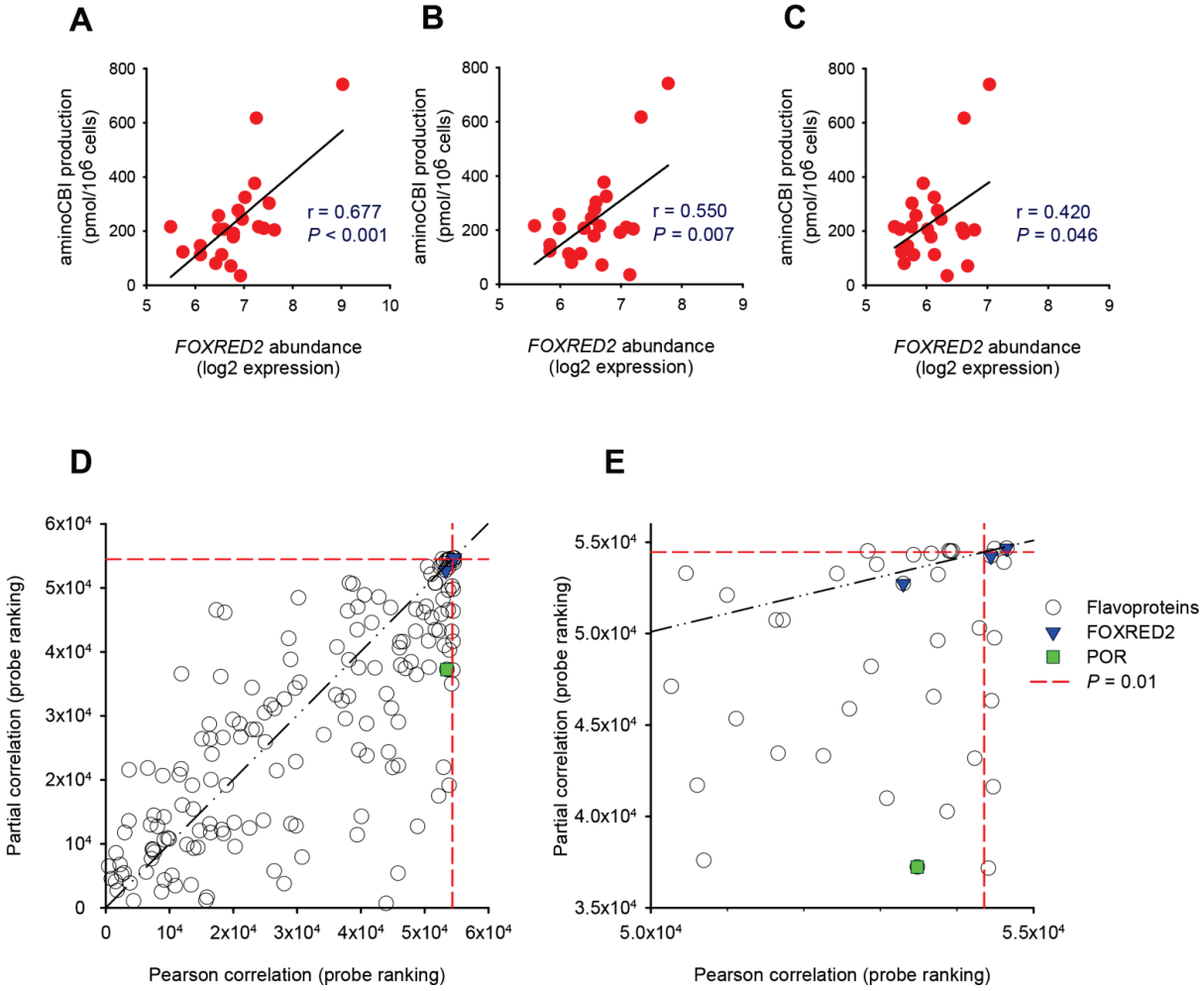

Figure 5: FOXRED2 expression increases activation and cytotoxicity of SN29428 under hypoxic conditions.

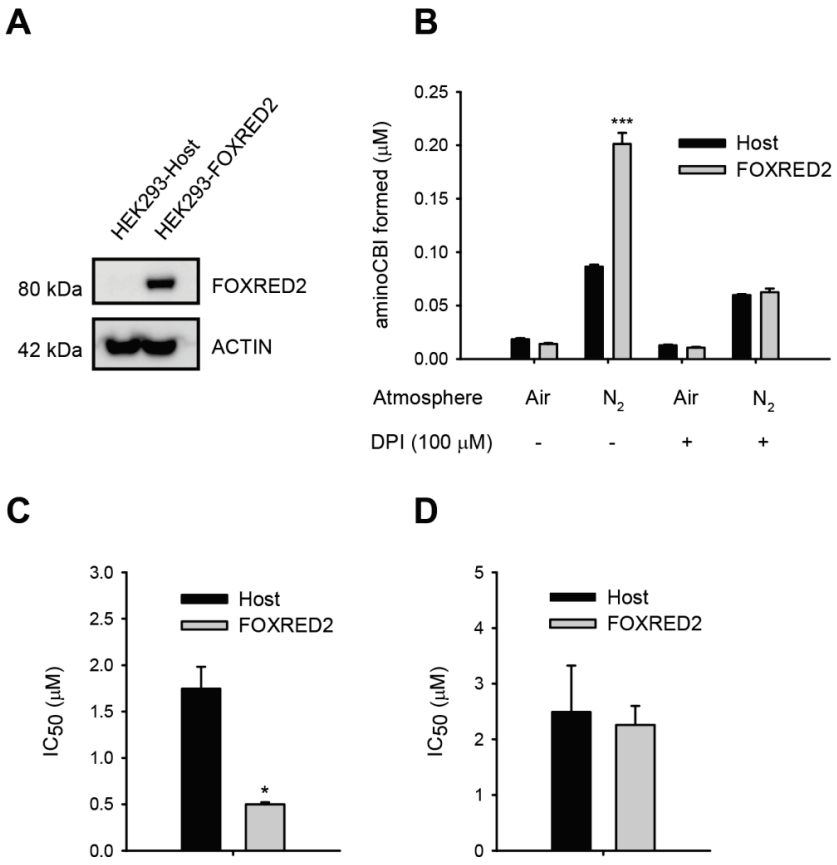

Figure 6: FOXRED2 activates the bioreductive prodrugs SN30000, TPZ and PR-104A and increases cell sensitivity to TH-302.